FERMILAB-PUB-07-395-E

Search for $B_s^0 \to \mu^+\mu^-$ decays at D0

V.M. Abazov[35], B. Abbott[75], M. Abolins[65], B.S. Acharya[28], M. Adams[51], T. Adams[49], E. Aguilo[5], S.H. Ahn[30], M. Ahsan[59], G.D. Alexeev[35], G. Alkhazov[39], A. Alton[64,a], G. Alverson[63], G.A. Alves[2], M. Anastasoaie[34], L.S. Ancu[34], T. Andeen[53], S. Anderson[45], B. Andrieu[16], M.S. Anzelc[53], Y. Arnoud[13], M. Arov[60], M. Arthaud[17], A. Askew[49], B. Åsman[40], A.C.S. Assis Jesus[3], O. Atramentov[49], C. Autermann[20], C. Avila[7], C. Ay[23], F. Badaud[12], A. Baden[61], L. Bagby[52], B. Baldin[50], D.V. Bandurin[59], S. Banerjee[28], P. Banerjee[28], E. Barberis[63], A.-F. Barfuss[14], P. Bargassa[80], P. Baringer[58], J. Barreto[2], J.F. Bartlett[50], U. Bassler[16], D. Bauer[43], S. Beale[5], A. Bean[58], M. Begalli[3], M. Begel[71], C. Belanger-Champagne[40], L. Bellantoni[50], A. Bellavance[50], J.A. Benitez[65], S.B. Beri[26], G. Bernardi[16], R. Bernhard[22], L. Berntzon[14], I. Bertram[42], M. Besançon[17], R. Beuselinck[43], V.A. Bezzubov[38], P.C. Bhat[50], V. Bhatnagar[26], C. Biscarat[19], G. Blazey[52], F. Blekman[43], S. Blessing[49], D. Bloch[18], K. Bloom[67], A. Boehnlein[50], D. Boline[62], T.A. Bolton[59], G. Borissov[42], K. Bos[33], T. Bose[77], A. Brandt[78], R. Brock[65], G. Brooijmans[70], A. Bross[50], D. Brown[78], N.J. Buchanan[49], D. Buchholz[53], M. Buehler[81], V. Buescher[21], S. Burdin[42,b], S. Burke[45], T.H. Burnett[82], C.P. Buszello[43], J.M. Butler[62], P. Calfayan[24], S. Calvet[14], J. Cammin[71], S. Caron[33], W. Carvalho[3], B.C.K. Casey[77], N.M. Cason[55], H. Castilla-Valdez[32], S. Chakrabarti[17], D. Chakraborty[52], K.M. Chan[55], K. Chan[5], A. Chandra[48], F. Charles[18,‡], E. Cheu[45], F. Chevallier[13], D.K. Cho[62], S. Choi[31], B. Choudhary[27], L. Christofek[77], T. Christoudias[43,†], S. Cihangir[50], D. Claes[67], B. Clément[18], Y. Coadou[5], M. Cooke[80], W.E. Cooper[50], M. Corcoran[80], F. Couderc[17], M.-C. Cousinou[14], S. Crépé-Renaudin[13], D. Cutts[77], M. Ćwiok[29], H. da Motta[2], A. Das[62], G. Davies[43], K. De[78], S.J. de Jong[34], P. de Jong[33], E. De La Cruz-Burelo[64], C. De Oliveira Martins[3], J.D. Degenhardt[64], F. Déliot[17], M. Demarteau[50], R. Demina[71], D. Denisov[50], S.P. Denisov[38], S. Desai[50], H.T. Diehl[50], M. Diesburg[50], A. Dominguez[67], H. Dong[72], L.V. Dudko[37], L. Duflot[15], S.R. Dugad[28], D. Duggan[49], A. Duperrin[14], J. Dyer[65], A. Dyshkant[52], M. Eads[67], D. Edmunds[65], J. Ellison[48], V.D. Elvira[50], Y. Enari[77], S. Eno[61], P. Ermolov[37], H. Evans[54], A. Evdokimov[73], V.N. Evdokimov[38], A.V. Ferapontov[59], T. Ferbel[71], F. Fiedler[24], F. Filthaut[34], W. Fisher[50], H.E. Fisk[50], M. Ford[44], M. Fortner[52], H. Fox[22], S. Fu[50], S. Fuess[50], T. Gadfort[82], C.F. Galea[34], E. Gallas[50], E. Galyaev[55], C. Garcia[71], A. Garcia-Bellido[82], V. Gavrilov[36], P. Gay[12], W. Geist[18], D. Gelé[18], C.E. Gerber[51], Y. Gershtein[49], D. Gillberg[5], G. Ginther[71], N. Gollub[40], B. Gómez[7], A. Goussiou[55], P.D. Grannis[72], H. Greenlee[50], Z.D. Greenwood[60], E.M. Gregores[4], G. Grenier[19], Ph. Gris[12], J.-F. Grivaz[15], A. Grohsjean[24], S. Grünendahl[50], M.W. Grünewald[29], J. Guo[72], F. Guo[72], P. Gutierrez[75], G. Gutierrez[50], A. Haas[70], N.J. Hadley[61], P. Haefner[24], S. Hagopian[49], J. Haley[68], I. Hall[65], R.E. Hall[47], L. Han[6], K. Hanagaki[50], P. Hansson[40], K. Harder[44], A. Harel[71], R. Harrington[63], J.M. Hauptman[57], R. Hauser[65], J. Hays[43], T. Hebbeker[20], D. Hedin[52], J.G. Hegeman[33], J.M. Heinmiller[51], A.P. Heinson[48], U. Heintz[62], C. Hensel[58], K. Herner[72], G. Hesketh[63], M.D. Hildreth[55], R. Hirosky[81], J.D. Hobbs[72], B. Hoeneisen[11], H. Hoeth[25], M. Hohlfeld[21], S.J. Hong[30], R. Hooper[77], S. Hossain[75], P. Houben[33], Y. Hu[72], Z. Hubacek[9], V. Hynek[8], I. Iashvili[69], R. Illingworth[50], A.S. Ito[50], S. Jabeen[62], M. Jaffré[15], S. Jain[75], K. Jakobs[22], C. Jarvis[61], R. Jesik[43], K. Johns[45], C. Johnson[70], M. Johnson[50], A. Jonckheere[50], P. Jonsson[43], A. Juste[50], D. Käfer[20], S. Kahn[73], E. Kajfasz[14], A.M. Kalinin[35], J.R. Kalk[65], J.M. Kalk[60], S. Kappler[20], D. Karmanov[37], J. Kasper[62], P. Kasper[50], I. Katsanos[70], D. Kau[49], R. Kaur[26], V. Kaushik[78], R. Kehoe[79], S. Kermiche[14], N. Khalatyan[38], A. Khanov[76], A. Kharchilava[69], Y.M. Kharzheev[35], D. Khatidze[70], H. Kim[31], T.J. Kim[30], M.H. Kirby[34], M. Kirsch[20], B. Klima[50], J.M. Kohli[26], J.-P. Konrath[22], M. Kopal[75], V.M. Korablev[38], A.V. Kozelov[38], D. Krop[54], A. Kryemadhi[81], T. Kuhl[23], A. Kumar[69], S. Kunori[61], A. Kupco[10], T. Kurča[19], J. Kvita[8], F. Lacroix[12], D. Lam[55], S. Lammers[70], G. Landsberg[77], J. Lazoflores[49], P. Lebrun[19], W.M. Lee[50], A. Leflat[37], F. Lehner[41], J. Lellouch[16], J. Leveque[45], P. Lewis[43], J. Li[78], Q.Z. Li[50], L. Li[48], S.M. Lietti[4], J.G.R. Lima[52], D. Lincoln[50], J. Linnemann[65], V.V. Lipaev[38], R. Lipton[50], Y. Liu[6,†], Z. Liu[5], L. Lobo[43], A. Lobodenko[39], M. Lokajicek[10], A. Lounis[18], P. Love[42], H.J. Lubatti[82], A.L. Lyon[50], A.K.A. Maciel[2], D. Mackin[80], R.J. Madaras[46], P. Mättig[25], C. Magass[20], A. Magerkurth[64], N. Makovec[15], P.K. Mal[55], H.B. Malbouisson[3], S. Malik[67], V.L. Malyshev[35], H.S. Mao[50], Y. Maravin[59], B. Martin[13], R. McCarthy[72], A. Melnitchouk[66], A. Mendes[14], L. Mendoza[7], P.G. Mercadante[4], M. Merkin[37], K.W. Merritt[50], J. Meyer[21], A. Meyer[20], M. Michaut[17], T. Millet[19], J. Mitrevski[70], J. Molina[3], R.K. Mommsen[44], N.K. Mondal[28], R.W. Moore[5], T. Moulik[58], G.S. Muanza[19], M. Mulders[50], M. Mulhearn[70], O. Mundal[21], L. Mundim[3], E. Nagy[14], M. Naimuddin[50], M. Narain[77], N.A. Naumann[34], H.A. Neal[64], J.P. Negret[7], P. Neustroev[39], H. Nilsen[22], A. Nomerotski[50],

S.F. Novaes[4], T. Nunnemann[24], V. O'Dell[50], D.C. O'Neil[5], G. Obrant[39], C. Ochando[15], D. Onoprienko[59], N. Oshima[50], J. Osta[55], R. Otec[9], G.J. Otero y Garzón[51], M. Owen[44], P. Padley[80], M. Pangilinan[77], N. Parashar[56], S.-J. Park[71], S.K. Park[30], J. Parsons[70], R. Partridge[77], N. Parua[54], A. Patwa[73], G. Pawloski[80], B. Penning[22], K. Peters[44], Y. Peters[25], P. Pétroff[15], M. Petteni[43], R. Piegaia[1], J. Piper[65], M.-A. Pleier[21], P.L.M. Podesta-Lerma[32,d], V.M. Podstavkov[50], Y. Pogorelov[55], M.-E. Pol[2], P. Polozov[36], A. Pompoˇ, B.G. Pope[65], A.V. Popov[38], C. Potter[5], W.L. Prado da Silva[3], H.B. Prosper[49], S. Protopopescu[73], J. Qian[64], A. Quadt[21,e], B. Quinn[66], A. Rakitine[42], M.S. Rangel[2], K. Ranjan[27], P.N. Ratoff[42], P. Renkel[79], S. Reucroft[63], P. Rich[44], M. Rijssenbeek[72], I. Ripp-Baudot[18], F. Rizatdinova[76], S. Robinson[43], R.F. Rodrigues[3], C. Royon[17], P. Rubinov[50], R. Ruchti[55], G. Safronov[36], G. Sajot[13], A. Sánchez-Hernández[32], M.P. Sanders[16], A. Santoro[3], G. Savage[50], L. Sawyer[60], T. Scanlon[43], D. Schaile[24], R.D. Schamberger[72], Y. Scheglov[39], H. Schellman[53], P. Schieferdecker[24], T. Schliephake[25], C. Schwanenberger[44], A. Schwartzman[68], R. Schwienhorst[65], J. Sekaric[49], S. Sengupta[49], H. Severini[75], E. Shabalina[51], M. Shamim[59], V. Shary[17], A.A. Shchukin[38], R.K. Shivpuri[27], D. Shpakov[50], V. Siccardi[18], V. Simak[9], V. Sirotenko[50], P. Skubic[75], P. Slattery[71], D. Smirnov[55], J. Snow[74], G.R. Snow[67], S. Snyder[73], S. Söldner-Rembold[44], L. Sonnenschein[16], A. Sopczak[42], M. Sosebee[78], K. Soustruznik[8], M. Souza[2], B. Spurlock[78], J. Stark[13], J. Steele[60], V. Stolin[36], A. Stone[51], D.A. Stoyanova[38], J. Strandberg[64], S. Strandberg[40], M.A. Strang[69], M. Strauss[75], E. Strauss[72], R. Ströhmer[24], D. Strom[53], L. Stutte[50], S. Sumowidagdo[49], P. Svoisky[55], A. Sznajder[3], M. Talby[14], P. Tamburello[45], A. Tanasijczuk[1], W. Taylor[5], P. Telford[44], J. Temple[45], B. Tiller[24], F. Tissandier[12], M. Titov[17], V.V. Tokmenin[35], T. Toole[61], I. Torchiani[22], T. Trefzger[23], D. Tsybychev[72], B. Tuchming[17], C. Tully[68], P.M. Tuts[70], R. Unalan[65], S. Uvarov[39], L. Uvarov[39], S. Uzunyan[52], B. Vachon[5], P.J. van den Berg[33], B. van Eijk[33], R. Van Kooten[54], W.M. van Leeuwen[33], N. Varelas[51], E.W. Varnes[45], I.A. Vasilyev[38], M. Vaupel[25], P. Verdier[19], L.S. Vertogradov[35], M. Verzocchi[50], F. Villeneuve-Seguier[43], P. Vint[43], P. Vokac[9], E. Von Toerne[59], M. Voutilainen[67,f], M. Vreeswijk[33], R. Wagner[68], H.D. Wahl[49], L. Wang[61], M.H.L.S Wang[50], J. Warchol[55], G. Watts[82], M. Wayne[55], M. Weber[50], G. Weber[23], A. Wenger[22,g], N. Wermes[21], M. Wetstein[61], A. White[78], D. Wicke[25], G.W. Wilson[58], S.J. Wimpenny[48], M. Wobisch[60], D.R. Wood[63], T.R. Wyatt[44], Y. Xie[77], S. Yacoob[53], R. Yamada[50], M. Yan[61], T. Yasuda[50], Y.A. Yatsunenko[35], K. Yip[73], H.D. Yoo[77], S.W. Youn[53], J. Yu[78], A. Zatserklyaniy[52], C. Zeitnitz[25], D. Zhang[50], T. Zhao[82], B. Zhou[64], J. Zhu[72], M. Zielinski[71], D. Zieminska[54], A. Zieminski[54], L. Zivkovic[70], V. Zutshi[52], and E.G. Zverev[37]

(The DØ Collaboration)

[1] *Universidad de Buenos Aires, Buenos Aires, Argentina*
[2] *LAFEX, Centro Brasileiro de Pesquisas Físicas, Rio de Janeiro, Brazil*
[3] *Universidade do Estado do Rio de Janeiro, Rio de Janeiro, Brazil*
[4] *Instituto de Física Teórica, Universidade Estadual Paulista, São Paulo, Brazil*
[5] *University of Alberta, Edmonton, Alberta, Canada, Simon Fraser University, Burnaby, British Columbia, Canada, York University, Toronto, Ontario, Canada, and McGill University, Montreal, Quebec, Canada*
[6] *University of Science and Technology of China, Hefei, People's Republic of China*
[7] *Universidad de los Andes, Bogotá, Colombia*
[8] *Center for Particle Physics, Charles University, Prague, Czech Republic*
[9] *Czech Technical University, Prague, Czech Republic*
[10] *Center for Particle Physics, Institute of Physics, Academy of Sciences of the Czech Republic, Prague, Czech Republic*
[11] *Universidad San Francisco de Quito, Quito, Ecuador*
[12] *Laboratoire de Physique Corpusculaire, IN2P3-CNRS, Université Blaise Pascal, Clermont-Ferrand, France*
[13] *Laboratoire de Physique Subatomique et de Cosmologie, IN2P3-CNRS, Universite de Grenoble 1, Grenoble, France*
[14] *CPPM, IN2P3-CNRS, Université de la Méditerranée, Marseille, France*
[15] *Laboratoire de l'Accélérateur Linéaire, IN2P3-CNRS et Université Paris-Sud, Orsay, France*
[16] *LPNHE, IN2P3-CNRS, Universités Paris VI and VII, Paris, France*
[17] *DAPNIA/Service de Physique des Particules, CEA, Saclay, France*
[18] *IPHC, Université Louis Pasteur et Université de Haute Alsace, CNRS, IN2P3, Strasbourg, France*
[19] *IPNL, Université Lyon 1, CNRS/IN2P3, Villeurbanne, France and Université de Lyon, Lyon, France*
[20] *III. Physikalisches Institut A, RWTH Aachen, Aachen, Germany*
[21] *Physikalisches Institut, Universität Bonn, Bonn, Germany*
[22] *Physikalisches Institut, Universität Freiburg, Freiburg, Germany*

[23] *Institut für Physik, Universität Mainz, Mainz, Germany*
[24] *Ludwig-Maximilians-Universität München, München, Germany*
[25] *Fachbereich Physik, University of Wuppertal, Wuppertal, Germany*
[26] *Panjab University, Chandigarh, India*
[27] *Delhi University, Delhi, India*
[28] *Tata Institute of Fundamental Research, Mumbai, India*
[29] *University College Dublin, Dublin, Ireland*
[30] *Korea Detector Laboratory, Korea University, Seoul, Korea*
[31] *SungKyunKwan University, Suwon, Korea*
[32] *CINVESTAV, Mexico City, Mexico*
[33] *FOM-Institute NIKHEF and University of Amsterdam/NIKHEF, Amsterdam, The Netherlands*
[34] *Radboud University Nijmegen/NIKHEF, Nijmegen, The Netherlands*
[35] *Joint Institute for Nuclear Research, Dubna, Russia*
[36] *Institute for Theoretical and Experimental Physics, Moscow, Russia*
[37] *Moscow State University, Moscow, Russia*
[38] *Institute for High Energy Physics, Protvino, Russia*
[39] *Petersburg Nuclear Physics Institute, St. Petersburg, Russia*
[40] *Lund University, Lund, Sweden, Royal Institute of Technology and Stockholm University, Stockholm, Sweden, and Uppsala University, Uppsala, Sweden*
[41] *Physik Institut der Universität Zürich, Zürich, Switzerland*
[42] *Lancaster University, Lancaster, United Kingdom*
[43] *Imperial College, London, United Kingdom*
[44] *University of Manchester, Manchester, United Kingdom*
[45] *University of Arizona, Tucson, Arizona 85721, USA*
[46] *Lawrence Berkeley National Laboratory and University of California, Berkeley, California 94720, USA*
[47] *California State University, Fresno, California 93740, USA*
[48] *University of California, Riverside, California 92521, USA*
[49] *Florida State University, Tallahassee, Florida 32306, USA*
[50] *Fermi National Accelerator Laboratory, Batavia, Illinois 60510, USA*
[51] *University of Illinois at Chicago, Chicago, Illinois 60607, USA*
[52] *Northern Illinois University, DeKalb, Illinois 60115, USA*
[53] *Northwestern University, Evanston, Illinois 60208, USA*
[54] *Indiana University, Bloomington, Indiana 47405, USA*
[55] *University of Notre Dame, Notre Dame, Indiana 46556, USA*
[56] *Purdue University Calumet, Hammond, Indiana 46323, USA*
[57] *Iowa State University, Ames, Iowa 50011, USA*
[58] *University of Kansas, Lawrence, Kansas 66045, USA*
[59] *Kansas State University, Manhattan, Kansas 66506, USA*
[60] *Louisiana Tech University, Ruston, Louisiana 71272, USA*
[61] *University of Maryland, College Park, Maryland 20742, USA*
[62] *Boston University, Boston, Massachusetts 02215, USA*
[63] *Northeastern University, Boston, Massachusetts 02115, USA*
[64] *University of Michigan, Ann Arbor, Michigan 48109, USA*
[65] *Michigan State University, East Lansing, Michigan 48824, USA*
[66] *University of Mississippi, University, Mississippi 38677, USA*
[67] *University of Nebraska, Lincoln, Nebraska 68588, USA*
[68] *Princeton University, Princeton, New Jersey 08544, USA*
[69] *State University of New York, Buffalo, New York 14260, USA*
[70] *Columbia University, New York, New York 10027, USA*
[71] *University of Rochester, Rochester, New York 14627, USA*
[72] *State University of New York, Stony Brook, New York 11794, USA*
[73] *Brookhaven National Laboratory, Upton, New York 11973, USA*
[74] *Langston University, Langston, Oklahoma 73050, USA*
[75] *University of Oklahoma, Norman, Oklahoma 73019, USA*
[76] *Oklahoma State University, Stillwater, Oklahoma 74078, USA*
[77] *Brown University, Providence, Rhode Island 02912, USA*
[78] *University of Texas, Arlington, Texas 76019, USA*
[79] *Southern Methodist University, Dallas, Texas 75275, USA*
[80] *Rice University, Houston, Texas 77005, USA*
[81] *University of Virginia, Charlottesville, Virginia 22901, USA and*
[82] *University of Washington, Seattle, Washington 98195, USA*

(Dated: July 26, 2007)

We report results from a search for the decay $B_s^0 \to \mu^+\mu^-$ using 1.3 fb^{-1} of $p\overline{p}$ collisions at

$\sqrt{s} = 1.96$ TeV collected by the D0 experiment at the Fermilab Tevatron Collider. We find two candidate events, consistent with the expected background of 1.24 ± 0.99, and set an upper limit on the branching fraction of $\mathcal{B}(B_s^0 \to \mu^+\mu^-) < 1.2 \times 10^{-7}$ at the 95% C.L.

PACS numbers: 13.20.He, 12.15.Mm, 12.60.Jv, 13.85.Qk

The branching fraction $\mathcal{B}(B_s^0 \to \mu^+\mu^-)$ is predicted to be $(3.4 \pm 0.5) \times 10^{-9}$ [1] within the standard model (SM), where the decay occurs through helicity and CKM-suppressed processes involving multiple electroweak boson exchanges. In supersymmetric (SUSY) models, interactions with neutral Higgs bosons can enhance the branching ratio by several orders of magnitude if the value of $\tan\beta$, the ratio of vacuum expectation values for the two neutral CP-even Higgs fields, is high [2, 3, 4, 5, 6]. Large enhancements to $\mathcal{B}(B_s^0 \to \mu^+\mu^-)$ are possible in SUSY models with R-parity violating couplings even if $\tan\beta$ is low [7]. Improvements to the limit on $\mathcal{B}(B_s^0 \to \mu^+\mu^-)$ will constrain the parameter space of such models. The best published experimental bound is $\mathcal{B}(B_s^0 \to \mu^+\mu^-) < 2.0 \times 10^{-7}$ at the 95% C.L. [8]. The analysis reported in this letter used 1.3 fb^{-1} of $p\overline{p}$ collisions collected by the D0 experiment at the Fermilab Tevatron. It supercedes our previous result [9] based on a 240 pb^{-1} subsample of the data.

The D0 detector [10] features a three layer muon system [11] with each layer consisting of a scintillator plane and a three or four plane drift chamber, providing coverage for $\eta < |2|$, where $\eta = -\ln[\tan(\theta/2)]$, and θ is the polar angle with respect to the beamline. Muon backgrounds are low due to shielding from 1.8 T iron toroids located between the first and second muon detector layers, and from a 6–10 interaction length deep uranium/liquid-argon calorimeter located in front of the first layer. Charged particles are detected in the inner central tracking system, which consists of a silicon microstrip tracker (SMT) and a central fiber tracker (CFT), both located within a 2 T superconducting solenoidal magnet. The CFT has eight thin coaxial barrels, each supporting two doublets of overlapping scintillating fibers of 0.835 mm diameter, one doublet being parallel to the beam axis, and the other alternating by $\pm 3^\circ$. The SMT has four layers of double sided detectors divided into six longitudinal sections interspersed with sixteen radial disks. Each layer has a side with strips parallel to the beam axis; two layers have a $\pm 2^\circ$ stereo side, and two layers have a 90° side. Typical strip pitch is $50 - 80$ μm.

Events were recorded using a set of single muon triggers, dimuon triggers, and triggers that selected $p\overline{p}$ interactions based on energy depositions in the calorimeter. $B_s^0 \to \mu^+\mu^-$ [12] candidates were formed from pairs of oppositely charged muons. Each muon was required to have transverse momentum $p_T > 2.5$ GeV, and to have hits in at least two layers of the muon system, four layers of the CFT, and three layers of the SMT. The B_s^0 candidate was required to have $p_T > 5$ GeV. There is a large background due primarily to muons from the decay of pions, kaons, and b- or c- flavored hadrons. The $B_s^0 \to \mu^+\mu^-$ signal is characterized by the long lifetime of the B_s^0, which results in an observable distance between the point at which the B_s^0 is produced (the primary vertex) and the point at which it decays. The distance from the primary vertex to the B_s^0 vertex in the transverse plane (L_T) was required to have an uncertainty $\sigma_{L_T} < 0.015$ cm and a significance $L_T/\sigma_{L_T} > 12$. The average L_T for signal events passing the p_T requirement is ~ 0.1 cm. Typically σ_{L_T} is between 0.002 and 0.009 cm for both signal and background. The angle between the projections onto the transverse plane of the B_s^0 momentum and the displacement from the primary vertex to the B_s^0 vertex was required to be less than 15°. The distance of closest approach δ of each muon to the primary vertex in the transverse plane was calculated, along with the corresponding uncertainty σ_δ and significance δ/σ_δ. The smaller of the two significances, $\min(\delta/\sigma_\delta)$, was required to be greater than 2.8. This removes a class of events in which one of the tracks is consistent with originating from the primary vertex. A constrained fit was applied, enforcing the conditions that the tracks making up the B_s^0 intersect in space and the three dimensional B_s^0 trajectory pass through the primary vertex. The fit probability $P(\chi^2)$ is the fraction of the area of the χ^2 distribution that lies below the χ^2 value returned by the constrained fit. It was required to be at least 0.01.

To further suppress the background, a likelihood ratio test was applied. Five variables were incorporated:

1. isolation, defined as $p_T^B/(p_T^B + \sum p_T)$ where p_T^B is the transverse momentum of the B_s^0 system, and $\sum p_T$ is the scalar sum of the transverse momenta of all other tracks within a cone of $\Delta R < 1$ around the B_s^0 system, where $\Delta R = \sqrt{(\Delta\phi)^2 + (\Delta\eta)^2}$ and ϕ is the azimuthal angle
2. $P(\chi^2)$
3. L_T/σ_{L_T}
4. $\min(\delta/\sigma_\delta)$
5. $m_{\mu\mu}$, the mass of the dimuon system.

The likelihood ratio was approximated as $r = \prod_{i=1}^{5} S_i/B_i$ where S_i is the probability distribution of the ith variable for the signal, and B_i is the distribution for the background. The discriminant $D_5 = r/(1+r)$ takes a value between zero (background-like) and one (signal-like). Figure 1 shows the distributions of S_i and B_i for isolation and for functions of

L_T/σ_{L_T}, $\min(\delta/\sigma_\delta)$, and $P(\chi^2)$. The functions map the quantities into the range zero to one. They are given by $f_1(L_T/\sigma_{L_T}) = 1 - \exp[-0.057(L_T/\sigma_{L_T} - 12)]$, $f_2[\min(\delta/\sigma_\delta)] = 1 - \exp[-0.093(\min(\delta/\sigma_\delta) - 2.8)]$, and $f_3[P(\chi^2)] = (P(\chi^2) - 0.01)/0.99$. In Fig. 1, the signal and background events satisfy all of the preselection cuts defined earlier except for the cut on L_T significance. To increase the statistics, the L_T significance cut was relaxed from twelve to five. The signal distributions S_i are given by the histograms in Fig. 1. These distributions are the result of Monte Carlo (MC) simulations using the PYTHIA event generator [13] interfaced with the EVTGEN decay package [14], followed by full GEANT v3.15 [15] modeling of the detector response. The simulation was tuned to reproduce the momentum resolution and scale, the trigger efficiency, and the B^+ meson p_T distribution observed in data. The MC events were processed with the same event reconstruction used for the data. The background distributions B_i are given by parameterizations of the sideband data, shown in Fig. 1. The sideband data consist of candidates having a dimuon invariant mass $m_{\mu\mu}$ between 4.5 and 7.0 GeV excluding the signal region. The signal region is between 4.972 and 5.717 GeV, approximately ± 3 standard deviations around the mean of the Gaussian $m_{\mu\mu}$ distribution in the signal MC. The sideband isolation distribution was fit to a Gaussian function, and the other three sideband distributions were fit to the sum of two exponential functions. The $m_{\mu\mu}$ distribution of the background was approximated to be flat when computing the likelihood ratio. The distribution of D_5 for signal and background is shown in Fig. 2. Final candidates were required to have $m_{\mu\mu}$ within the signal region and to satisfy $D_5 > 0.949$. This threshold was chosen to optimize the expected 95% C.L. upper bound on $\mathcal{B}(B_s^0 \to \mu^+\mu^-)$. Two candidates pass the final selection.

An important feature of the background is seen in Fig. 3, which shows the distribution of $m_{\mu\mu}$ after various cuts, beginning with the L_T significance cut and ending with $D_4 > 0.949$. The discriminant D_4 was calculated in the same way as D_5 except that the variable $m_{\mu\mu}$ was omitted, thereby simulating the effect of a cut on D_5 without biasing the $m_{\mu\mu}$ distribution toward the B_s^0 mass. Two components are evident in the distributions: a steeply falling component in the low mass region and a gradually falling component whose slope diminishes as the cuts tighten. This structure was studied using $b\bar{b}$ events generated with PYTHIA, which reproduced the main features of the data. The contributions from particles misidentified as muons and other sources of real muons are small. The gradually falling component consists of events in which the two muons arise from the decay of separate b quarks, while the steeply falling component consists of events in which the two muons arise from decay of the same b quark, via sequential decay $b \to c\mu\nu$ followed by $c \to s\mu\nu$ or from $b \to \psi' X$ with $\psi' \to \mu\mu$. Higher mass ψ' states may also contribute

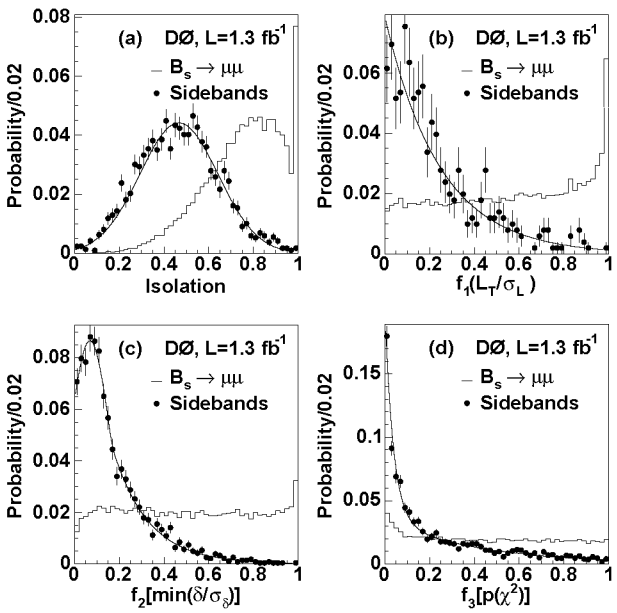

FIG. 1: Signal and background distributions for four of the variables used in the likelihood ratio test. The signal distributions are from MC, and the background distributions are from the sideband data. The sideband distribution in (a) is parameterized as a Gaussian function. In (b), (c), and (d), the sideband distributions are parameterized as the sum of two exponential functions.

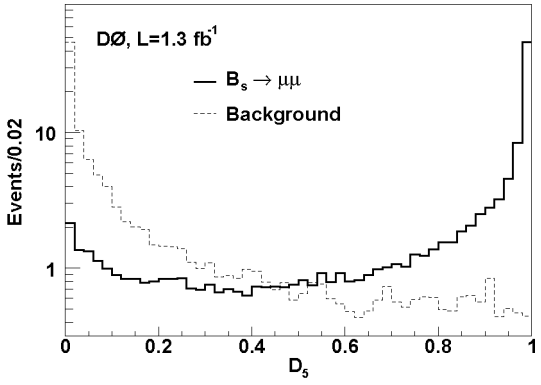

FIG. 2: The distribution of discriminant D_5 for signal and background. The background distribution is derived from events in the sidebands, folded over possible values of $m_{\mu\mu}$ in the signal region. The signal distribution is from MC. The normalization of the MC is arbitrary.

in the data. Because the same-b processes result from a single b quark, they have a better chance of producing a dimuon system that forms a common vertex and points back to the primary vertex than do the separate-b processes.

The expected number of background events in the final candidate sample was estimated using events from the data in the low and high sidebands, together with the as-

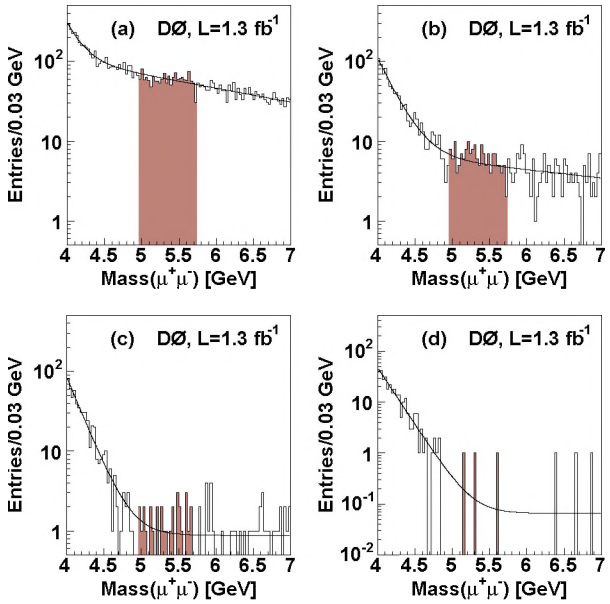

FIG. 3: The dimuon mass distribution at different stages in a sequence of cuts: (a) after $L_T > 12\sigma_{L_T}$, (b) after $\min(\delta/\sigma_\delta) > 2.8$ and $P(\chi^2) > 0.01$, (c) after $D_4 > 0.5$, and (d) after $D_4 > 0.949$. In (a) and (b) the histograms are fit to the sum of two exponential functions, while in (c) and (d) they are fit to the sum of an exponential and a constant. The signal region (shaded) was excluded in the fits. In (d), three entries are included in the signal region: the entry near the upper bound of the signal region has a value of D_4 close to the threshold and fails the D_5 cut; the other two entries are the final candidates.

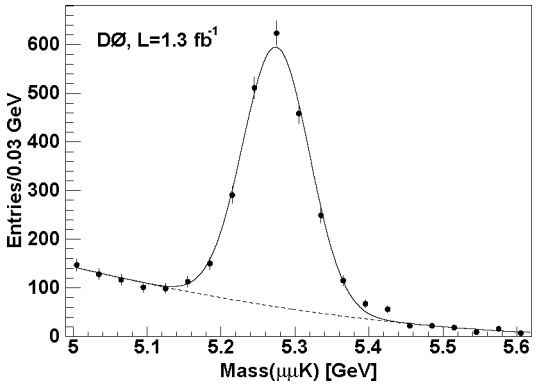

FIG. 4: Mass distribution of B^+ candidates. The background distribution is parameterized as a parabola and the signal distribution as a Gaussian function.

sumption that the background consists of same-b events having an exponential mass distribution and separate-b events having a flat mass distribution. This model of the shape of the backgrounds fits the sideband regions well and accurately predicts the number of events in the signal region, see Fig. 3. The slope of the exponential was taken from the fit in Fig. 3(d). The fits in Figs. 3(c) and (d) are consistent with a flat distribution for separate-b events. The separate-b distribution might still decrease gradually with mass after a cut on D_4, but the slope is not well constrained by the statistics in the high sideband, and to neglect it is conservative in its effect on the branching fraction limit. Given the number of events in the low sideband and the slope of the exponential, the expected contribution of same-b events to the high sideband is negligible. The estimated background from separate-b events is $\sum_i P_i \cdot w$ where the sum is over all events in the high sideband. The variable w is the expected number of separate-b events in the signal region per separate-b event in the high sideband, determined from the range of the signal region, the range of the high sideband region, and the shape of the mass distribution for separate-b events. The variable P_i is the probability for a separate-b event to pass the cut $D_5 > 0.949$ given that it falls within the signal region and has the specific value of D_4 observed for the ith event in the high sideband. This probability was determined by integrating over the possible mass values in the signal region. Likewise, the background from same-b events was computed using the corresponding sum over events in the low sideband. However, the low sideband contains separate-b events as well as same-b events. As a result, the low sideband sum is an overestimate of the same-b background. The contribution due to separate-b events in the low sideband was estimated using the high sideband data and subtracted. The total estimated background is $1.24 \pm 0.99 \pm 0.08$ events, where the first uncertainty is statistical and the second is due to the uncertainty in the shape of the $m_{\mu\mu}$ distribution.

The branching fraction was obtained by normalizing to the number of $B^+ \to J/\psi K^+ \to \mu^+\mu^- K^+$ candidates observed in the data. B^+ candidates were formed in a similar fashion to the B_s^0 candidates, but with the addition of a third track, which was assumed to be a kaon and required to have $p_T > 1.0$ GeV. The three tracks had to form a common vertex, and the two muons had to have a mass near the J/ψ mass. As with B_s^0 candidates, the muon pair was required to have $\min(\delta/\sigma_\delta) > 2.8$. The B^+ system had to pass the same p_T, angle, σ_{L_T}, L_T/σ_{L_T}, and $P(\chi^2)$ cuts as the B_s^0 system. Finally, the B^+ system was required to have $D_4 > 0.949$. The number of B^+ decays $n_{B^+} = 2016 \pm 55\,(\text{stat}) \pm 45\,(\text{syst})$ was determined from the fit to the reconstructed mass distribution shown in Fig. 4.

The branching fraction is related to n_{B^+} by

$$\begin{aligned} \mathcal{B}(B_s^0 \to \mu^+\mu^-) \;=\; & \frac{n_{B_s^0}}{n_{B^+}} \cdot \frac{\epsilon_{B^+}}{\epsilon_{B_s^0}} \cdot \frac{f(\bar{b} \to B^+)}{f(\bar{b} \to B_s^0)} \\ & \times\; \mathcal{B}(B^+ \to J/\psi K^+) \cdot \mathcal{B}(J/\psi \to \mu^+\mu^-), \end{aligned} \tag{1}$$

which is obtained by eliminating the integrated luminosity and b quark production cross section from the expressions for the B^+ and B_s^0 yields. The quantity $n_{B_s^0}$ is the number of $B_s^0 \to \mu^+\mu^-$ decays observed in

the data. The efficiencies ϵ_{B^+} and $\epsilon_{B_s^0}$ are, respectively, the fractions of $B^+ \to J/\psi K^+ \to \mu^+\mu^- K^+$ decays and $B_s^0 \to \mu^+\mu^-$ decays that are observed in the MC. The ratio $\epsilon_{B^+}/\epsilon_{B_s^0}$ is 0.172 ± 0.015, where the sources of uncertainty include the dimuon mass resolution and scale, the shape of the discriminant distribution, trigger efficiency, MC statistics, and the shape of the p_T distribution for B_s^0 and B^+. The B meson production ratio was calculated to be $\frac{f(\bar{b}\to B^+)}{f(\bar{b}\to B_s^0)} = 3.86 \pm 0.54$ from the production fractions of Refs. [16, 17] and the correlation coefficient from Ref. [17]. The branching fractions $\mathcal{B}(B^+ \to J/\psi K^+) = (1.008 \pm 0.035) \times 10^{-3}$ and $\mathcal{B}(J/\psi \to \mu^+\mu^-) = 0.0593 \pm 0.0006$ are from Ref. [16]. The product of the factors multiplying $n_{B_s^0}$ on the right hand side of Eq. 1 is therefore $k = \mathcal{B}(B_s^0 \to \mu^+\mu^-)/n_{B_s^0} = (1.97 \pm 0.34) \times 10^{-8}$, often called the single event sensitivity. The contributions of the various sources of uncertainty to the relative uncertainty in k are listed in Table I.

Source	$\Delta k/k$
Mass resolution	0.007
Mass scale	0.013
Discriminant distribution	0.030
Trigger efficiency	0.007
MC statistics	0.024
B meson p_T spectrum	0.080
$f(\bar{b} \to B^+)/f(\bar{b} \to B_s^0)$	0.140
$\mathcal{B}(B^+ \to J/\psi K^+)$	0.035
$\mathcal{B}(J/\psi \to \mu^+\mu^-)$	0.010
B^+ fit (stat)	0.027
B^+ fit (syst)	0.022
Combined	0.17

TABLE I: Sources of uncertainty and their contributions to the relative uncertainty in the single event sensitivity k.

Uncertainties due to differences between the data and MC largely cancel in the ratio $\epsilon_{B^+}/\epsilon_{B_s^0}$, although not completely. For instance, muons from $B_s^0 \to \mu^+\mu^-$ decay mostly have higher p_T than muons from $B^+ \to J/\psi K^+ \to \mu^+\mu^- K^+$ decay, in which the energy is shared among three particles. The resulting effect on the efficiency of the trigger and muon p_T cuts depends on the p_T distribution of the parent B mesons, and the shape of this distribution is the dominant source of uncertainty in $\epsilon_{B^+}/\epsilon_{B_s^0}$. The extra track in B^+ decays together with better tracking and vertexing in the MC than in the data result in an overestimate of $\epsilon_{B^+}/\epsilon_{B_s^0}$ and a slight worsening of the limit. The uncertainty due to modeling of the first four likelihood variables was estimated to be 3% based on a comparison between B^+ data and MC. The uncertainties due to the mass resolution (0.7%) and scale (1.3%) were estimated by comparing the $\Upsilon(1S) \to \mu^+\mu^-$ mass distribution in data and MC. Other uncertainties in $\epsilon_{B^+}/\epsilon_{B_s^0}$ are MC statistics (2.4%) and trigger efficiency (0.7%).

Given two candidates observed in the data, an upper limit on $n_{B_s^0}$ was computed taking into account the expected background and uncertainties using a Bayesian method. The resulting upper limit on the branching fraction is $\mathcal{B}(B_s^0 \to \mu^+\mu^-) < 1.2 \times 10^{-7}$ at the 95% C.L. The expected limit is 0.97×10^{-7}. This result improves upon the best previously published upper bound for this branching fraction [8].

We thank the staffs at Fermilab and collaborating institutions, and acknowledge support from the DOE and NSF (USA); CEA and CNRS/IN2P3 (France); FASI, Rosatom and RFBR (Russia); CAPES, CNPq, FAPERJ, FAPESP and FUNDUNESP (Brazil); DAE and DST (India); Colciencias (Colombia); CONACyT (Mexico); KRF and KOSEF (Korea); CONICET and UBACyT (Argentina); FOM (The Netherlands); Science and Technology Facilities Council (United Kingdom); MSMT and GACR (Czech Republic); CRC Program, CFI, NSERC and WestGrid Project (Canada); BMBF and DFG (Germany); SFI (Ireland); The Swedish Research Council (Sweden); CAS and CNSF (China); Alexander von Humboldt Foundation; and the Marie Curie Program.

[1] A. J. Buras, Phys. Lett. B **566**, 115 (2003).
[2] K. S. Babu and C. F. Kolda, Phys. Rev. Lett. **84**, 228 (2000).
[3] S. R. Choudhury and N. Gaur, Phys. Lett. B **451**, 86 (1999).
[4] R. Dermisek, S. Raby, L. Roszkowski, and R. Ruiz De Austri, JHEP **04**, 037 (2003).
[5] T. Blazek, S. F. King, and J. K. Parry, Phys. Lett. B **589**, 39 (2004).
[6] D. Auto *et al.*, JHEP **06**, 023 (2003).
[7] R. Arnowitt, B. Dutta, T. Kamon, and M. Tanaka, Phys. Lett. B **538**, 121 (2002).
[8] A. Abulencia *et al.* (CDF Collaboration), Phys. Rev. Lett. **95**, 221805 (2005).
[9] V. M. Abazov *et al.* (D0 Collaboration), Phys. Rev. Lett. **94**, 071802 (2005).
[10] V. M. Abazov *et al.* (D0 Collaboration), Nucl. Instrum. Methods A **565**, 463 (2006).
[11] V. M. Abazov *et al.* (D0 Collaboration), Nucl. Instrum. Methods A **552**, 372 (2005).
[12] Charge conjugate states are included implicitly throughout this paper.
[13] T. Sjöstrand *et al.*, Comput. Phys. Commun. **135**, 238 (2001).
[14] D. J. Lange, Nucl. Instrum. Methods A **462**, 152 (2001).
[15] R. Brun and F. Carminati, CERN Program Library Long Writeup W5013 (unpublished).
[16] W.-M. Yao *et al.* (Particle Data Group), J. Phys. Lett. G **33**, 1 (2006).
[17] E. Barberio *et al.* (Heavy Flavor Averaging Group), `http://www.slac.stanford.edu/xorg/hfag/osc/PDG_2006/index.h`